Modulation of Phospholipase A_2 Activity by Aminoglycosides and Daptomycin: A Fourier Transform Infrared Spectroscopic Study†

Danielle Carrier,* Maroun Bou Khalil, and Alayne Kealey

Department of Biochemistry, Faculty of Medicine, University of Ottawa, 451 Smyth Road, Ottawa, Ontario, Canada K1H 8M5

Received July 23, 1997; Revised Manuscript Received March 13, 1998

ABSTRACT: The antibiotics known as aminoglycosides are commonly used to treat severe infections caused by Gram-negative bacteria. Unfortunately, they often lead to acute renal failure after their accumulation in the lysosomes of renal cells, where an inhibition of the phospholipid catabolism is observed. The lipopeptidic antibiotic daptomycin has been shown to reduce the nephrotoxicity of aminoglycosides, but the exact mechanism of this protection is still unknown. In the present study, Fourier transform infrared spectroscopy (FTIR) has been used to monitor the hydrolysis of phosphatidylcholine by phospholipase A_2 (PLA_2) from *Naja mocambique mocambique* venom in the presence of various aminoglycosides and/or daptomycin. Gentamicin and amikacin inhibited the reaction in its early stage. Kanamycin A, tobramycin, and especially kanamycin B *enhanced* the initial enzyme activity by reducing the lag time. After the initiation period, the reaction proceeded at a much slower rate in the presence of gentamicin. On the other hand, daptomycin led to dramatic alterations of the hydrolysis profile: the initial latency period was eliminated, and the maximal extent of hydrolysis was reduced. When both daptomycin and any of the aminoglycosides were present, the latency period also disappeared, and the phospholipase activity was higher than with the lipopeptide alone. The most drastic change occurred with gentamicin, which was the most inhibitory aminoglycoside when used alone but worked synergistically with daptomycin to yield the most dramatic activation of PLA_2.

Aminoglycoside antibiotics are hydrophilic, oligocationic molecules consisting of an aminocyclitol ring associated with an aminated sugar (Figure 1). These antibiotics are produced by two types of bacteria: *Micromonospora* and *Streptomyces* (*1*). They present a wide spectrum of action and are effective against most Gram-negative bacteria and certain Gram-positive bacteria (*2*). They kill bacteria by interfering with their protein synthesis at the initiation stage (*2*). Due to their rapid effectiveness and broad-spectrum activity, the aminoglycosides are among the most widely used antimicrobial agents (*3*). Unfortunately, their therapeutic use is complicated by the high incidence of nephrotoxicity (*4*). The mechanism underlying the latter is not fully understood, but its comprehension would greatly help in the design of less toxic structures.

Aminoglycosides are not metabolized and are mostly eliminated by the kidney glomerular filtration (*5*). They tend to accumulate in high concentrations in the proximal tubule cells during the subsequent reabsorption step (*5*−*7*). Owing to their positive charges, these drugs can interact with negatively charged membranes. Phosphatidylinositol has been proposed to be their receptor on brush border membranes (*8*). After binding, they are internalized by pinocytosis, followed by fusion of the endocytotic vacuoles with primary lysosomes where they accumulate and inhibit phospholipases and sphingomyelinase activity (*9*). This results in the formation and growth of myeloid bodies, until bursting of the lysosomes. Necrosis of tubular cells is then observed, together with an impairment of renal functions.

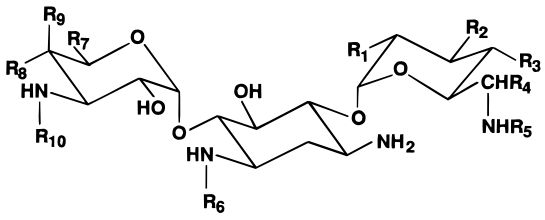

	R_1	R_2	R_3	R_4	R_5	R_6	R_7	R_8	R_9	R_{10}
kanamycin B	NH_2	OH	OH	H	H	H	CH_2OH	OH	H	H
kanamycin A	OH	OH	OH	H	H	H	CH_2OH	OH	H	H
amikacin	OH	OH	OH	H	H	HABA	CH_2OH	OH	H	H
tobramycin	NH_2	H	OH	H	H	H	CH_2OH	OH	H	H
gentamicin:										
C_1	NH_2	H	H	CH_3	CH_3	H	H	CH_3	OH	CH_3
C_2	NH_2	H	H	CH_3	H	H	H	CH_3	OH	CH_3
C_3	NH_2	H	H	H	H	H	H	CH_3	OH	CH_3

FIGURE 1: Chemical structure of the aminoglycosides used in this study. The name gentamicin generally designates a mixture of the three isomers C_1, C_2, and C_3 (or C_{1A}). HABA, *S*-4-amino-2-hydroxybutyryl.

† This work was supported by the Natural Sciences and Engineering Council of Canada.

* To whom correspondence should be addressed. Telephone: (613) 562-5800 (ext. 8215). Fax: (613) 562-5440. E-mail: carrier@uottawa.ca.

S0006-2960(97)01793-5 CCC: $15.00 © 1998 American Chemical Society
Published on Web 05/02/1998

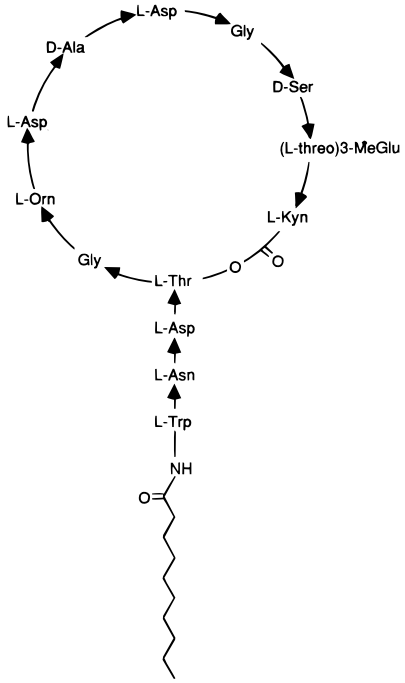

FIGURE 2: Chemical structure of daptomycin (formerly LY146032).

The lipopeptide daptomycin (Figure 2) shows a bactericidal activity against Gram-positive bacteria in which it inhibits the synthesis of lipoteichoic acid (*10*). Daptomycin has been shown to prevent the development of tobramycin-induced nephrotoxicity in rats (*11*, *12*). It inhibited lysosomal phospholipidosis and increased cellular regeneration in the presence of similar or even higher aminoglycoside levels (*11*, *12*). The mechanism underlying the nephroprotection afforded by daptomycin is still unknown. Immunogold labeling experiments showed that both daptomycin and tobramycin accumulate in the lysosomes of renal proximal tubular cells (*13*). Whereas dialysis results indicated electrostatic interactions between tobramycin and daptomycin in aqueous solution (*14*), a subsequent infrared spectroscopic study demonstrated that daptomycin does not impede the binding of aminoglycosides to negatively charged membranes (*15*). It was hypothesized that the protective action of daptomycin might be due to its effect on the physical properties of the phospholipid bilayers forming the myeloid bodies. Daptomycin affects the membrane charge density as well as the lipid packing, two parameters that influence the activity of phospholipases.

In the present study, Fourier transform infrared spectroscopy (FTIR)[1] was used to monitor the hydrolysis of a mixture of phospholipids by a well-known phospholipase, the phospholipase A_2 (or PLA_2) from *Naja mocambique mocambique*. The influence of five aminoglycosides on the hydrolysis profile was investigated, and the action of daptomycin was finally examined.

MATERIALS AND METHODS

The sulfate salts of amikacin, kanamycins A and B, gentamicin, and tobramycin, the sodium salt of L-α-phosphatidyl-DL-inositol from soya, 1,2-dipalmitoyl-3-*sn*-phosphatidylcholine, 1,2-dimyristoyl-3-*sn*-phosphatidylcholine, phospholipase A_2 from *Naja mocambique mocambique*, and TRIS−HCl were obtained from Sigma Chemical Co. (St. Louis, MO). Deuterated water was purchased from Aldrich Chemical Co. (Milwaukee, MI). Daptomycin (LY146032) was a generous gift of Eli-Lilly Canada (Scarborough, Canada).

Prior to hydrolysis experiments, the best lipidic composition had to be determined. The activity of PLA_2 is maximal when the membrane is close to its transition temperature (*16*). The infrared spectra of various mixtures were measured at increasing temperature in order to determine their transition temperature. Different lipidic mixtures of DMPC/DPPC/PI were prepared in glass vials by combining the required volumes of chloroform or chloroform/methanol (1:1, v/v) solutions of each lipid, drying under a stream of nitrogen, and leaving overnight under vacuum. The lipidic dispersions (10% w/v) for infrared measurements were prepared by hydrating the dry lipid mixtures with the appropriate amount of 400 mM TRIS, 10 mM $CaCl_2$ in ^2H_2O, p^{2}H 8.0. At least three freeze−thaw cycles were done to ensure a homogeneous organization of the bilayers (liposomes). If required, the pH was adjusted by adding minimal amounts of deuterated NaOH or HCl. The sample was transferred between two barium fluoride windows separated by a 6-μm spacer, and the spectra were recorded at increasing temperature on a Digilab FTS-40A with a spectral resolution of 2 cm^{-1}. A total of 256 interferograms were co-added for each spectrum. The data were processed with homemade software (*17*). The frequencies were determined with the aid of Fourier derivation (*18*).

For hydrolysis measurements, the appropriate amounts of aminoglycoside and/or daptomycin in buffered solutions were added to the lipidic dispersion, and additional freeze−thaw cycles were performed. The PI:aminoglycoside molar ratio was 2:1, and the PI:daptomycin molar ratio was 4:1. After the addition of the phospholipase, the sample was quickly transferred into the infrared cell and placed into the spectrometer. The infrared spectrum of the reaction mixture was recorded at various time intervals, under the conditions given above. Phospholipase A_2 cleaves specifically the ester bond of the *sn*-2 chain of zwitterionic phospholipids. According to Beer−Lambert law, the absorbance of the ester groups is directly proportional to their concentration. The consumption of the substrate can therefore be monitored directly from the intensity of the ester carbonyl stretching band, since the fatty acid produced has no contribution in that frequency range because it is ionized at pH 8.0. Alternatively, the hydrolysis can be followed using the emerging bands attributed to the product carboxylate groups. The reaction progress curves are given as the ratio of the integrated intensity of the total carboxylate stretching band (1525−1610 cm^{-1}) at a given time over the integrated intensity of the C−H stretching region (2810−3000 cm^{-1}). The total intensity of this latter depends directly on the initial number of phospholipid molecules in the sample, and this normalization allows comparisons of different experiments.

[1] Abbreviations: DMPC, dimyristoylphosphatidylcholine; DMPG, dimyristoylphosphatidylglycerol; DPPC, dipalmitoylphosphatidylcholine; PC, phosphatidylcholine; PI, phosphatidylinositol; PLA_2, phospholipase A_2; PLA_1, phospholipase A_1; FTIR, Fourier transform infrared spectroscopy.

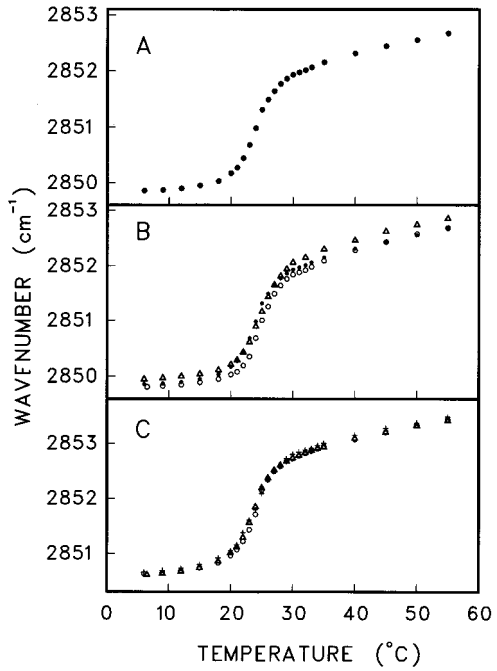

FIGURE 3: (A) Temperature dependence of the frequency of the symmetric C−H stretching vibration of the methylene groups of DMPC/DPPC/PI at a molar ratio of 8:1:1. (B) Temperature profile obtained in the presence of gentamicin (open circles) or of kanamycin B (open triangles), at a PI:aminoglycoside molar ratio of 2:1. The profile obtained in the absence of drugs is added for comparison (dots). (C) Temperature profile obtained for the same lipid mixture in the presence of daptomycin (4 PI:1 daptomycin) only (+) or with daptomycin and either gentamicin (open circles) or kanamycin B (open triangles), with a PI:aminoglycoside molar ratio of 2:1. All the samples were prepared in 400 mM TRIS, 10 mM $CaCl_2$ buffer in ^2H_2O, at p^{2}H 8.0. The frequencies were obtained after Fourier derivation of the original FTIR spectra with a power of 3 and a breakpoint of 0.3.

RESULTS

Physical State of the Lipid Mixture. The physical state of liposomal lipidic bilayers depends on temperature. In the fluid state, the lipid hydrocarbon chains are highly disordered, similarly to a long aliphatic hydrocarbon like hexadecane in the liquid phase. When the temperature is lowered, the chains have less energy to rotate about the C−C bonds, and they tend to get locked in the *all-trans* conformation, corresponding to a carbon skeleton extended in a perfect zigzag pattern. This *all-trans* structure is the conformation with the lowest energy, and it allows a very orderly packing of the chains, which maximizes their van der Waals interactions. Phospholipid bilayers in the gel state have their acyl chains in a mostly *all-trans* conformation. The frequency and shape of some infrared bands are sensitive to conformational changes in the lipid acyl chains, and these can be used to probe the membrane fluidity. The frequency of the methylene symmetric stretching band (2850 cm^{-1}) is known to increase with the number of gauche conformers in the acyl chains (*19*, *20*). A rapid increase of that frequency is observed at the transition temperature because of the important increase in the proportion of gauche bonds within the hydrocarbon chains (Figure 3). This higher conformational disorder accounts partly for the characteristic fluidity of the hydrophobic core of the bilayer in the fluid state. The gel-to-fluid transition of an 8:1:1 mixture of DMPC/DPPC/PI occurs at 23.6 °C (Figure 3A). The presence of a single transition is consistent with a homogeneous distribution of the different lipids in the bilayers.

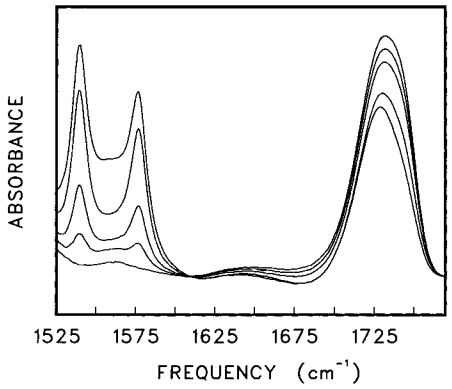

FIGURE 4: Carbonyl stretching region of the infrared spectrum of a dispersion of DMPC/DPPC/PI with a molar ratio of 8:1:1, at different time intervals (2−60 min) after the addition of phospholipase A_2. As the reaction progresses, the intensity of the ester carbonyl stretching band (at 1730 cm^{-1}) decreases, and new bands develop between 1520 and 1600 cm^{-1}. The samples were prepared in 400 mM TRIS, 10 mM $CaCl_2$ buffer in ^2H_2O, at p^{2}H 8.0.

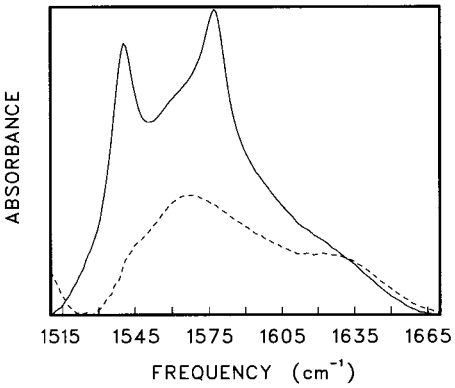

FIGURE 5: Carboxylate antisymmetric stretching region of the infrared spectrum of a dispersion of DMPC containing 10 mol % myristic acid, prepared in 400 mM TRIS buffer in ^2H_2O, p^{2}H 8.0, without calcium (dashed line) or with 10 mM $CaCl_2$ (solid line).

Hydrolysis of the Lipid Mixture. The enzyme phospholipase A_2 hydrolyzes specifically the ester bond of the *sn*-2 chain of zwitterionic phospholipids such as PC. For each PC molecule, one molecule of fatty acid and one molecule of lysophosphatidylcholine are produced. Since the reaction is performed at pH 8.0, the fatty acids are mostly under the carboxylate form, and their antisymmetric C═O stretching band is expected to be found at ca. 1560 cm^{-1}, far below the signal from the ester group of the reactant (*21*). The progress of the hydrolysis can be followed in Figure 4, where the intensity of the ester carbonyl stretching band (at 1733 cm^{-1}) falls down as a new set of bands builds up in the region 1520−1580 cm^{-1}. These new contributions are attributed to the carbonyl antisymmetric stretching vibration of the carboxylate groups, and they indicate the formation of myristate and palmitate ions in the sample. In the absence of calcium ions, a single and very broad band is observed at 1563 cm^{-1} for the antisymmetric stretching mode of the carboxylate group of myristic acid in a 10 mol % mixture with DMPC, dispersed in deuterated water (Figure 5, dashed line). The two carbon−oxygen bonds are equivalent and intermediate in strength between a single and a double bond. In the presence of 10 mM Ca^{2+}, two new peaks appear on

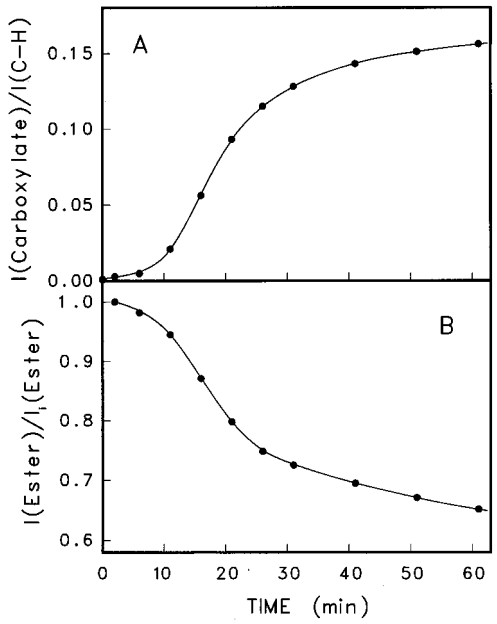

FIGURE 6: Reaction progress curve for PLA_2 hydrolysis of a dispersion of DMPC/DPPC/PI with a molar ratio of 8:1:1. In panel A, the ordinate represents the ratio of the total integrated intensity of the antisymmetric stretching bands of the product carboxylate groups (1525−1610 cm^{-1}) over the integrated intensity of the C−H stretching region (2810−3000 cm^{-1}). The curve in panel B represents the evolution of the integrated intensity of the ester carbonyl stretching band divided by the intensity measured at the beginning of the reaction. For both profiles, each data point is the average of the values obtained in three separate experiments. The samples were prepared in 400 mM TRIS, 10 mM $CaCl_2$ buffer in ^2H_2O, at p^{2}H 8.0.

top of that broad band, at 1577 and 1540 cm^{-1} (Figure 5, solid line). As reported by Deacon and Phillips (*22*), the frequencies of the asymmetric stretching vibration of carboxylate groups interacting with divalent metal cations vary according to the type of coordination: a downward shift indicates a bidentate coordination, a unidentate coordination gives an upward shift, and there is no significant change for bridging coordinations between one divalent cation and two oxygen atoms from distinct carboxylate groups. The bands at 1540 and 1577 cm^{-1} can therefore be attributed to carboxylate groups interacting with calcium ions in the bidentate and unidentate coordinations, respectively.

To get reaction progress curves, the carboxylate stretching region was integrated, and each intensity value was divided by the total integrated intensity of the C−H stretching region, which is proportional to the hydrocarbon concentration. The ratio obtained is directly proportional to the concentration of the products, and it is plotted against time (Figure 6A). This normalization makes possible the comparison of different samples and the averaging of similar experiments.

As mentioned in the previous section, the hydrolysis reaction can be monitored either from the product formation or from the substrate consumption. For comparison, the reactant disappearance curve in the absence of drugs is given in Figure 6B as a plot of the integrated intensity of the ester carbonyl band at a given time divided by the intensity measured at the beginning of the reaction. The general features of the two curves in Figure 6 are in very good agreement. To avoid redundancy, only the product formation curves are shown in Figures 7−9. The carboxylate region

Table 1: Gel to Liquid-Crystalline Transition Temperature of Dispersions of DMPC/DPPC/PI in a Molar Ratio of 8:1:1[a]

	transition temp (°C)	
aminoglycoside[b]	lipid	lipid + daptomycin[c]
none	23.6	23.4
gentamicin	24.3	24.0
amikacin	24.5	24.0
kanamycin A	24.4	24.0
kanamycin B	24.5	23.4
tobramycin	24.5	23.4

[a] Obtained from the methylene symmetric stretching vibration in the infrared spectrum. The lipidic dispersions were prepared in 400 mM TRIS, 10 mM $CaCl_2$ buffer in ^2H_2O, p^{2}H 8.0. [b] PI:aminoglycoside molar ratio of 2:1. [c] PI:daptomycin molar ratio of 4:1.

used to probe the fatty acid formation was found to be more accurate than the ester carbonyl band because the only correction required was for the spectral contribution of daptomycin.

The reaction progress curve for the DMPC/DPPC/PI mixture can be divided in three distinct regions (Figure 6). In the initial portion, the activity of PLA_2 is very low. This is called the latency period, or lag phase. Its duration depends on the quantity of enzyme, on the concentration of negatively charged lipids in the bilayer, and on the physical state of the latter. Although the hydrolysis is slow, it eventually yields enough product to change the enzyme kinetic parameters. The fatty acids produced give a higher charge density to the membrane, increasing the affinity of the enzyme in solution for the bilayer surface (*23*−*25*). In addition, the presence of lysophosphatidylcholine within the bilayer facilitates the catalytic step itself (*26*, *27*). The second portion of the reaction curve corresponds to fast hydrolysis (Figure 6). As the reactant disappears, the reaction eventually slows down and the curve forms a plateau, identified as the third region. The total decrease in intensity of the ester carbonyl band (Figure 6B) indicates that about 80% of the reactant has been hydrolyzed after 1 h.

Effect of Aminoglycosides and Daptomycin on the Physical State of the Lipid Mixture. The accumulation of aminoglycosides in the renal cortex is initiated by their binding to the negatively charged PI contained in the renal basolateral and brush border membranes. The temperature profile observed in the presence of gentamicin (Figure 3B, open circles) exhibits a single transition at a slightly higher temperature, 24.3 °C, compared to 23.6 °C for the lipid mixture alone. A transition temperature of approximately 24.5 °C was observed in the presence of amikacin, tobramycin, or kanamycins A or B (Table 1).

In the presence of daptomycin, the frequency of the methylene symmetric stretching vibration was about 1 cm^{-1} higher over all the temperature range (Figure 3C). This frequency change can be attributed to the spectral contribution of the lipopeptide. Daptomycin induced a shallow decrease of the transition midpoint, from 23.6 °C for the lipid alone to 23.4 °C with the lipopeptide (Figure 3C, +). In the presence of both gentamicin and daptomycin, the gel-to-fluid transition occurred at 24.0 °C (Figure 3C, open circles). Amikacin and kanamycin A both gave a transition temperature of 24.0 °C when combined with daptomycin, a temperature slightly *lower* than in the absence of daptomycin

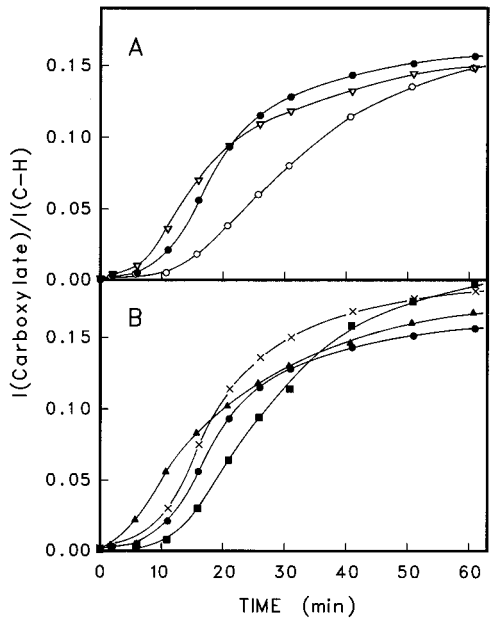

FIGURE 7: Reaction progress curve for PLA_2 hydrolysis of a dispersion of DMPC/DPPC/PI with a molar ratio of 8:1:1, in the absence (closed circles, $n = 3$) or in the presence of gentamicin (panel A, open circles, $n = 3$), tobramycin (panel A, open triangles, $n = 2$), amikacin (panel B, closed squares, $n = 3$), kanamycin B (panel B, closed triangles, $n = 4$), or kanamycin A (panel B, ×, $n = 2$). The ordinate represents the ratio of the total integrated intensity of the antisymmetric stretching bands of the product carboxylate groups (1525−1610 cm^{-1}) over the integrated intensity of the C−H stretching region (2810−3000 cm^{-1}). The samples were prepared in 400 mM TRIS, 10 mM $CaCl_2$ buffer in ^2H_2O, at p^{2}H 8.0. The PI:aminoglycoside molar ratio was 2:1.

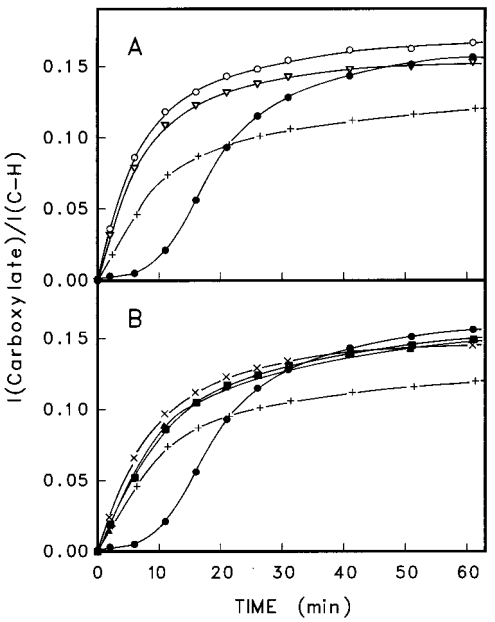

FIGURE 8: Reaction progress curve for PLA_2 hydrolysis of a dispersion of DMPC/DPPC/PI with a molar ratio of 8:1:1, in the absence (closed circles, $n = 3$) or in the presence of daptomycin (+, $n = 3$), at a PI:daptomycin molar ratio of 4:1. The other profiles were obtained in the presence of both daptomycin and gentamicin (panel A, open circles, $n = 2$), tobramycin (panel A, open triangles, $n = 2$), amikacin (panel B, closed squares, $n = 3$), kanamycin B (panel B, closed triangles, $n = 2$), or kanamycin A (panel B, ×, $n = 3$). The ordinate represents the ratio of the total integrated intensity of the antisymmetric stretching bands of the product carboxylate groups (1525−1610 cm^{-1}) over the integrated intensity of the C−H stretching region (2810−3000 cm^{-1}). The samples were prepared in 400 mM TRIS, 10 mM $CaCl_2$ buffer in ^2H_2O, at p^{2}H 8.0. The PI:aminoglycoside molar ratio was 2:1.

(see Table 1). For kanamycin B (Figure 3C, open triangles) and tobramycin (not shown), the addition of daptomycin resulted in a shift from 24.5 to 23.4 °C.

Neither daptomycin nor any of the aminoglycosides affected significantly the cooperativity of the transition. This indicates the absence of lateral phase separation within the lipidic bilayer, i.e., no formation of domains enriched with specific constituants.

Effect of Aminoglycosides on PLA_2 Activity. The reaction progress curves obtained in the presence of each of the aminoglycosides are plotted in Figure 7, together with that of the lipid mixture alone (closed circles). The effects observed include changes in the duration of the latency period and alterations of the final hydrolysis level. Gentamicin (panel A, open circles) and amikacin (panel B, closed squares) induced an increase of the latency period, but kanamycin A (panel B, ×), tobramycin (panel A, open triangles), and especially kanamycin B (panel B, closed triangles) reduced it. Kanamycin A and amikacin gave higher product concentrations in their plateau regions, whereas tobramycin and gentamicin had the opposite effect.

Effect of Daptomycin on PLA_2 Activity. Daptomycin inserts readily into phospholipidic bilayers (*15*), due to the hydrophobicity of its acyl chain (Figure 2). It was proposed that it might protect against aminoglycoside nephrotoxicity by restoring the membrane physical characteristics required for optimal phospholipase activity (*15*). As seen in Figure 8, the initial latency period is eliminated in the presence of daptomycin (+), but the hydrolysis rate remains lower than that of the pure lipidic mixture (closed circles) and the maximal extent of hydrolysis is much lower.

Effect of Aminoglycosides on PLA_2 Activity in the Presence of Daptomycin. Daptomycin also suppressed the latency period in the presence of aminoglycosides (Figure 8), and all the curves have a simple rectangular hyperbolic shape. Whereas gentamicin could be identified as the most inhibitory in Figure 7 (panel A, open circles), its combination with daptomycin (Figure 8A, open circles) allowed faster hydrolysis than for the lipid mixture alone (Figure 8A, closed circles) or for the lipid mixture with daptomycin (Figure 8, +). In the presence of any other aminoglycoside, the final extent of hydrolysis was slightly reduced compared to the lipid mixture alone, but still much higher than with only daptomycin.

DISCUSSION

The overall catalytic cycle of phospholipase A_2 occurs in two distinct steps. First, the enzyme in the aqueous phase becomes activated as it binds to the membrane surface (*28*). This activation step is promoted by the presence of negatively charged lipids in the membrane. The activated enzyme then binds a molecule of substrate phospholipid at the catalytic site to give the Michaelis complex which proceeds on to generate the hydrolysis products and the free enzyme (*29*). Secreted phospholipases A_2 require the presence of a calcium ion as a cofactor in their catalytic site. Ca^{2+} binds to the reactant and stabilizes the transition state (*30*, *31*). A second calcium binding site, with a lower affinity, seems to be associated with a 5−10-fold activation of the enzyme (*32*). Depending on the conditions, the reaction products may

enhance the hydrolysis rate when they reach a critical concentration (*33*). The initial slow hydrolysis period is then called the latency period.

Several lipophilic compounds reduce the rate of lipid hydrolysis by decreasing the phospholipase affinity for the interface. Upon binding to the bilayer, such inhibitors affect its physical properties in a way that promotes the desorption of the bound enzyme (*34*). It also appears that any physical or chemical change leading to an increase in membrane curvature enhances PLA_2 activity, usually by decreasing the latency period. Hence, no lag time is observed with sonicated vesicles, which have a small diameter (*35*). The high curvature allows an easier access of the enzyme to the substrate and therefore shifts the equilibrium for the second step of the mechanism toward the products. A high curvature is not an absolute requirement for promoting the hydrolysis reaction. Hence, cone-shaped lipids such as cardiolipin or diacylglycerol were shown to enhance the activity of various PLA_2s (*36*). Diacylglycerol, even at low concentrations (2−10 mol %), reduces the latency period (*23*). Yet, a study of a range of diacylglycerols revealed that their incorporation into PC bilayers results in a *decrease* of the area per phospholipid molecule and an *increase* in the lateral surface pressure (*37*). The effect of diacylglycerol on PLA_2 was therefore proposed to be related to its ability to promote lipid lateral segregation into domains (*16*, *37*).

PLA_2 indeed prefers laterally segregated bilayers. Using fluorescently marked PLA_2, Grainger and co-workers (*38*) have shown that the enzyme initially binds mostly to the fluid phase of a PC monolayer and then attacks its substrate exclusively at the gel−fluid transition region. This explains the early finding that the hydrolytic activity of pancreatic phospholipase A_2 increases dramatically in the vicinity of the lipid gel-to-fluid transition temperature, where gel state domains coexist with fluid phase domains (*39*). Hønger et al. recently reported that the lag time is smaller under conditions for which there is a high proportion of the bilayer surface that corresponds to borders between gel and fluid regions (*40*). Therefore, a bilayer having a broad transition is expected to promote the enzyme activity because of the smaller size of the cooperative units.

The rate enhancement caused by the product lysophospholipid is believed to result from the formation of defects in the bilayer surface (*27*). The fatty acids would work in synergism with the lysophospholipid as they promote lateral phase separation (*24*, *25*, *41*). The fatty acids also increase the negative charge of the bilayer, enhancing the affinity of the enzyme for the interface and therefore promoting its activation.

Since the nephrotoxicity of aminoglycoside antibiotics is always accompanied by a reduction of the lysosomal phospholipid catabolism, their inhibitory potency on phospholipases has been examined. Carlier et al. (*42*) found that both lysosomal phospholipases A_1 and A_2 were inhibited by various aminoglycosides after their binding to PI-containing liposomes. PI was required for both the binding of the aminoglycosides and their inhibition of PLA_2 as well as PLA_1. The inhibitory concentrations of aminoglycosides for PLA_2 and PLA_1 were similar, and the inhibitory potency order was sisomycin ≥ dibekacin ≈ gentamicin (mixture or C_1, C_{1a}, or C_2 alone) ≈ tobramycin or kanamycin B > netilmycin > kanamycin A or HABA-dibekacin > amikacin > octamethylkanamycin A or tetramethylkanamycin A > streptomycin. The inhibition was found to be directly related to the extent of aminoglycoside binding, at least for streptomycin, amikacin, and gentamicin. It was concluded that the higher inhibitory potency of gentamicin simply results from its higher binding.

Our hydrolysis profiles exhibit major differences among the various aminoglycosides investigated (Figure 7). Since we were using saturating proportions of drugs (only two PI molecules per aminoglycoside), a complete neutralization of the lipidic charges is expected, and it can be assumed that the differences do not result from inequivalent binding. In the absence of any drug, the lipid mixture exhibits a single and cooperative transition from the gel to the fluid state (Figure 3A). This indicates a complete mixing of the components and the absence of lateral phase segregation. Since the activity of the enzyme is maximal at the frontier between gel and fluid regions, the hydrolysis experiments were performed at a temperature corresponding to ∼50−75% completion of the transition. The initial state of the bilayer was monitored using the frequency of the methylene symmetric stretching vibration.

In the presence of an aminoglycoside, an increase of approximately 1 °C of the lipid gel-to-fluid transition temperature was observed (Table 1). This increase of the transition temperature results from the neutralization of the charges of PI, which allows a closer interaction between the lipid molecules and therefore favors the gel phase. Similar increases of the transition temperature have been reported as a result of the neutralization of the negative charges of a bilayer consisting only of an anionic phospholipid. Slight increases of 0.7−1.2 °C were reported for dimyristoylphosphatidylglycerol (DMPG) after the binding of amikacin or kanamycins A or B (*43*).

As seen in Figure 3B, the temperature profiles obtained in the presence of either kanamycin B or gentamicin contain a single transition whose cooperativity is not affected significantly. The five aminoglycosides yielded very similar profiles. This single, cooperative transition indicates that the lipid bilayer behaves as a homogeneous entity and that the drug does not induce any perceptible lateral phase separation.

Under these conditions, and despite the similarities in their structures, amikacin and kanamycin B had drastically different effects on the enzyme activity over the initial 30-min period (Figure 7B). Amikacin increased substantially the latency period whereas kanamycin B almost eliminated it. Kanamycin B appears to induce a distinctive type of bilayer perturbation, very conducive to the catalytic step. This perturbation is sufficient to counterbalance the expected decrease of the enzyme affinity for the bilayer caused by the neutralization of its negative charges. Interestingly, a recent investigation of the effects of amikacin and kanamycins A and B on DMPG liposomes led to the conclusion that amikacin is likely to be simply electrostatically adsorbed on the surface of the bilayer whereas kanamycin B would intercalate between the headgroups, giving rise to a more important perturbation of the interface (*43*). This suggests that similarly to lysophospholipids, kanamycin B creates surface defects that promote the catalytic step. The longer latency period obtained with amikacin is also completely consistent with the description given above. Amikacin does

not introduce any disruption of the lipidic network; the headgroup neutralization simply increases the cohesion of the lipid bilayer, which is detrimental to the lytic action of the enzyme. The larger reaction yield obtained after 1 h in the presence of amikacin and kanamycins A and B (Figure 7B), compared to the lipid mixture alone, could be due to the neutralization of the fatty acids produced, delaying the inhibitive action of the latter. The inhibitory potency of the two hydrolysis products was demonstrated in a careful kinetic study by Wells (*44*). At low concentration, fatty acids promote the activation of the enzyme, but they become noncompetitive inhibitors at higher concentrations (*45*).

Gentamicin, on the other hand, is the aminoglycoside that inhibited most efficiently the enzyme in the initial stage (Figure 7A). Carlier et al. (*42*) also found it to be a more potent inhibitor of lysosomal phospholipases than any of the other aminoglycosides investigated in the present study. As mentioned earlier, gentamicin is not produced by *Streptomyces* bacteria but by *Micromonospora*, and it therefore belongs to a different family. From a glance at the table on Figure 1, one can see that gentamicins contain more hydrophobic methyl substituants and fewer hydroxyl groups. Gentamicin is therefore less likely to simply lay on the bilayer surface, like amikacin. The higher hydrophobicity of gentamicin favors a deeper insertion toward the bilayer interior. The important increase of the lag time suggests that gentamicin is buried sufficiently deeply to let the choline and inositol groups interact freely with the solvent. In other words, the inclusion of this aminoglycoside does not result in any appreciable disruption of the bilayer surface. However, a slight reduction of the mean area per phospholipid is expected to result from the neutralization of PI charges, and the higher cohesion of the lipid network should give lower hydrolysis rates. The effect of gentamicin on the hydrolysis profile is compared in Figure 7A with that of tobramycin, an aminoglycoside with the same number of ionizable amino groups and a size similar to that of gentamicin. Unlike the latter, tobramycin induced a decrease in the lag time. Being more hydrophilic, tobramycin would remain closer to the surface and create disruptions of the bilayer surface.

Owing to its amphiphilic character, daptomycin inserts readily into lipidic bilayers. It was found to induce a decrease of 5 °C of the transition temperature of DMPG, and of 7 °C for DPPC (*15*). The transition temperature of our lipid mixture was not altered significantly (Figure 3C). The transition remained single and as cooperative. Daptomycin molecules are expected to disperse within the lipid bilayer and stay as far as possible one from another due to the presence of many charges on each daptomycin peptidic moiety.

Daptomycin induced the elimination of the lag period (Figure 8A, +). The multiple aspartate side chains are likely to increase the affinity of the enzyme for the bilayer and should therefore favor the activation step of the enzyme. The effect of daptomycin on the catalytic step was difficult to predict. On one hand, the lipopeptide was reported to induce a slight tightening of the lipid interface at the level of the ester groups (*15*), which should play against the hydrolytic step. On the other hand, it also modifies the dynamics of common acyl chains because of the shortness of the hydrocarbon chain of daptomycin, which makes the central portion of the hydrophobic core more disordered (*15*, *46*). Overall, daptomycin had only a very small effect on the thermotropic behavior of the lipid mixture (Figure 3C). As stated above, the hydrolysis was performed under conditions corresponding to a 50−75% "melted" bilayer because PLA_2 is known to attack the lipids at the border between gel and fluid regions. Since daptomycin does not alter the transition cooperativity, the size of the cooperative units remains the same and, consequently, the proportion of lipid molecules located in the contact zones between different homogeneous regions is also unaffected. It is difficult to say, however, if daptomycin perturbs the availability of the phosphatidylcholine molecules in the border zones.

In addition to its charge, the shape of daptomycin could play a significant role in the activation phenomenon. With its bulky peptidic ring and its single acyl chain, the lipopeptide resembles an inverted cone, similarly to a lysophospholipid. It could therefore also promote the catalytic step by acting as a prong.

Daptomycin also limits the extent of hydrolysis. The final concentration of products is reduced by approximately 25%. The negatively charged lipopeptide probably acts as a noncompetitive inhibitor in the same way as the product fatty acid at high concentration (*45*).

The combination of daptomycin with any of our aminoglycosides induced the elimination of the latency period (Figure 8). The affinity of daptomycin for bilayers containing anionic lipids increases in the presence of gentamicin, and vice versa (*15*). This suggests that even in the presence of aminoglycosides, the insertion of daptomycin creates defects that promote the catalytic step. In a fluorescence study, Lakey and Ptak (*47*) showed that the lipopeptide penetrates further into phosphatidylcholine bilayers in the presence of calcium ions, which bind and neutralize the negatively charged side chains of daptomycin. They also noticed that the calcium effect was lessened when negatively charged lipids were added to the zwitterionic phospholipid, blurring the local negative potential due to daptomycin and necessary for the capture of the calcium ions.

In our experiments, the initial hydrolysis rates were particularly high for the more hydrophobic aminoglycosides, namely, gentamicin and tobramycin (Figure 8A). The dramatic synergy between daptomycin and gentamicin (Figure 9, closed triangles) could be explained by a deeper penetration of the more hydrophobic gentamicin/daptomycin complex into the bilayer. The complexation with gentamicin increases the disproportion between the cross section of the lipopeptide headgroup and that of its acyl chain. Due to its larger size and more hydrophilic character, amikacin cannot work as synergistically with daptomycin in enhancing the enzyme activity. Yet, as seen in Figure 8B, amikacin (closed squares) and kanamycin B (closed triangles) had very little effect on the initial hydrolysis rate in the presence of daptomycin. The differences between amikacin and the two kanamycins become less important in the presence of daptomycin.

The results presented here give additional insight into the behavior of secreted PLA_2 and represent a very important step toward our understanding of the mechanism for the nephroprotective action of daptomycin. As seen in the Discussion, the variations observed among the modulatory effects of the five aminoglycosides studied are directly related to their chemical structure. The number of charges, the size,

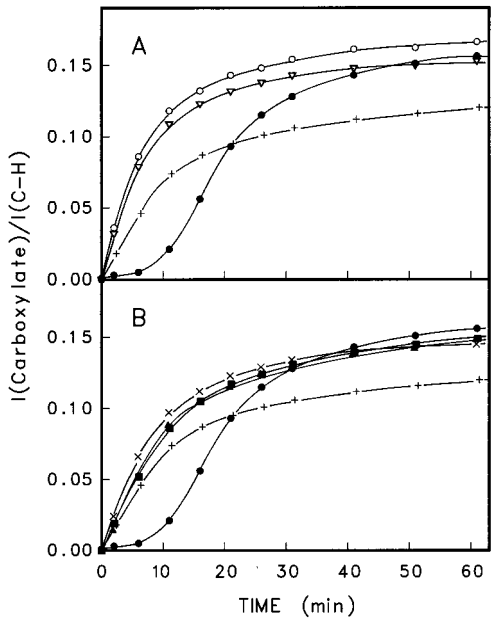

FIGURE 9: Reaction progress curve for PLA_2 hydrolysis of a dispersion of DMPC/DPPC/PI with a molar ratio of 8:1:1, in the absence of any drug (closed circles, $n = 3$) or in the presence of daptomycin only (+, $n = 3$), or of gentamicin only (open circles, $n = 3$), or of both daptomycin and gentamicin (closed triangles, $n = 2$). The ordinate represents the ratio of the total integrated intensity of the carboxylate antisymmetric stretching bands (1525−1610 cm^{-1}) over the integrated intensity of the C−H stretching region (2810−3000 cm^{-1}). The samples were prepared in 400 mM TRIS, 10 mM $CaCl_2$ buffer in ^2H_2O, at p^{2}H 8.0. The PI:drug molar ratio was 2:1 for gentamicin and 4:1 for daptomycin.

and especially the hydrophobicity of the substituents of an aminoglycoside determine its influence on the lag phase, on the maximal rate, and on the final extent of hydrolysis. Paradoxically, the aminoglycoside with the highest inhibitory potential against PLA_2 became the best activator when combined with daptomycin, despite the fact that the lipopeptide alone behaves as an inhibitor beyond the enzyme activation step.

ACKNOWLEDGMENT

We are indebted to Drs. Denis Beauchamp and Christian Salesse for helpful discussions. Dr. Beauchamp also provided samples of daptomycin. The technical assistance of Ms. Julie Souligny is acknowledged. We are also grateful to Ms. Pascale Eid for performing some preliminary work. A.K. thanks the School of Graduate Studies of the University of Ottawa for a research assistant scholarship.

REFERENCES

1. Nagabhushan, T. L., Miller, G. H., and Weinstein, M. J. (1982) in *The Aminoglycosides; Microbiology, Clinical Use and Toxicology* (Whelton, A., and Neu, H. C., Eds.) p 4, Marcel Dekker, Inc., New York.
2. Spelman, D. W., McDonald, M., and Spicer, W. J. (1989) *Med. J. Austr. 151*, 346−349.
3. Ali, B. H. (1995) *Gen. Pharmacol. 26*, 1477−1487.
4. Tulkens, P. M. (1989) *Toxicol. Lett. 46*, 107−123.
5. Bennett, W. M. (1989) *Clin. Exp. Pharmacol. Physiol. 16*, 1−6.
6. Pastoriza-Munoz, E., Bowman, R. L., and Kaloyanides, G. J. (1979) *Kidney Int. 16*, 440−450.
7. Silverblatt, F. J., and Kuehn, C. (1979) *Kidney Int. 15*, 335−345.
8. Sastrasinh, M., Knauss, T. C., Weinberg, J. M., and Humes, H. D. (1982) *J. Pharmacol. Exp. Ther. 222*, 350−358.
9. Laurent, G., Carlier, M. B., Rollman, B., Van Hoof, F., and Tulkens, P. (1982) *Biochem. Pharmacol. 31*, 3861−3870.
10. Canepari, P., Boaretti, M., Mar Lleó, M. D., and Salta, G. (1990) *Antimicrob. Agents Chemother. 34*, 1220−1226.
11. Wood, C. A., Finkbeiner, H. C., Kohlhepp, S. J., Kohnen, P. W., and Gilbert, D. N. (1989) *Antimicrob. Agents Chemother. 33*, 1280−1285.
12. Beauchamp, D., Pellerin, M., Gourde, P., Pettigrew, M., and Bergeron, M. G. (1990) *Antimicrob. Agents Chemother. 34*, 139−147.
13. Beauchamp, P., Gourde, P., Simard, M., and Bergeron, M. G. (1994) *Antimicrob. Agents Chemother. 38*, 189−194.
14. Couture, M., Simard, M., Gourde, P., Lessard, C., Gurnani, K., Carrier, D., Bergeron, M. G., and Beauchamp, D. (1994) *Antimicrob. Agents Chemother. 38*, 742−749.
15. Gurnani, K., Khouri, H., Couture, M., Bergeron, M. G., Beauchamp, D., and Carrier, D. (1995) *Biochim. Biophys. Acta 1237*, 86−94.
16. Bell, J. D., Burnside, M., Owen, J. A., Royall, M. L., and Baker, M. L. (1996) *Biochemistry 35*, 4945−4955.
17. Cameron, D. G., and Moffatt, D. J. (1984) *J. Test. Eval. 12*, 78−85.
18. Cameron, D. G., and Moffatt, D. J. (1987) *Appl. Spectrosc. 41*, 539−544.
19. Casal, H. L., and Mantsch, H. H. (1984) *Biochim. Biophys. Acta 779*, 381−401.
20. Umemura, J., Cameron, D. G., and Mantsch, H. H. (1980) *Biochim. Biophys. Acta 602*, 32−44.
21. Colthup, N. B., Daly, L. H., and Wiberley, S. E. (1990) *Introduction to Infrared and Raman Spectroscopy*, 3rd ed., pp 318 and 390, Academic Press, San Diego.
22. Deacon, G. B., and Phillips, R. J. (1980) *Coord. Chem. Rev. 33*, 227−250.
23. Bell, J. D., Baker, M. L., Bent, E. D., Ashton, R. W., Hemming, D. J. B., and Hansen, L. D. (1995) *Biochemistry 34*, 11551−11560.
24. Bent, E. D., and Bell, J. D. (1995) *Biochim. Biophys. Acta 1254*, 349−360.
25. Jain, M. K., Yu, B.-Z., and Kozubek, A. (1989a) *Biochim. Biophys. Acta 980*, 23−32.
26. Gelb, M. H., Jain, M. K., Hanel, A. M., and Berg, O. G. (1995) *Annu. Rev. Biochem. 64*, 653−688.
27. Sheffield, M. J., Baker, B. L., Li, D., Owen, N. L., Baker, M. L., and Bell, J. D. (1995) *Biochemistry 34*, 7796−7806.
28. Gelb, M. H., Jain, M. K., and Berg, O. G. (1994) *FASEB J. 8*, 916−924.
29. Ghomashchi, F., O'Hare, T., Clary, D., and Gelb, M. H. (1991) *Biochemistry 30*, 7298−7305.
30. Scott, D. L., White, S. P., Otwinowski, Z., Yuan, W., Gelb, M. H., and Sigler, P. B. (1990) *Science 250*, 1541−1546.
31. Yu, B.-Z., Berg, O. G., and Jain, M. K. (1993) *Biochemistry 32*, 6485−6492.
32. Mezna, M., Ahmad, T., Chettibi, S., Drainas, D., and Lawrence, A. J. (1994) *Biochem. J. 301*, 503−508.
33. Jain, M. K., Egmond, M. R., Verheij, H. M., Apitz-Castro, R., Dijkman, R., and de Haas, G. H. (1982) *Biochim. Biophys. Acta 688*, 341−348.
34. Jain, M. K., Yuan, W., and Gelb, M. H. (1989b) *Biochemistry 28*, 4135−4139.
35. Menashe, M., Lichtenberg, D., Gutierrez-Merino, C., and Biltonen, R. L. (1981) *J. Biol. Chem. 256*, 4541−4543.
36. Buckley, J. J. (1985) *Can. J. Biochem. Cell Biol. 63*, 263−267.
37. De Boeck, H., and Zidovetski, R. (1992) *Biochemistry 31*, 623−630.
38. Grainger, D. W., Reichert, A., Ringsdorf, H., and Salesse, C. (1989) *FEBS Lett. 252*, 73−82.
39. Op den Kamp, J. A. F., de Gier, J., and van Deenen, L. L. M. (1974) *Biochim. Biophys. Acta 345*, 253−256.
40. Hønger, T., Jørgensen, K., Biltonen, R. L., and Mouritsen, O. G. (1996) *Biochemistry 35*, 9003−9006.

41. Burack, W. R., Yuan, Q., and Biltonen, R. L. (1993) *Biochemistry 32*, 583−589.
42. Carlier, M. B., Laurent, G., Claes, P. J., Vanderhaeghe, H. J., and Tulkens, P. M. (1983) *Antimicrob. Agents Chemother. 23*, 440−449.
43. Carrier, D., Chartrand, N., and Matar, W. (1997) *Biochem. Pharmacol. 53*, 401−408.
44. Wells, M. A. (1972) *Biochemistry 11*, 1030−1041.
45. Jain, M. K., and Jahagirdar, D. V. (1985) *Biochim. Biophys. Acta 914*, 319−326.
46. Eid, P., Wong, P. T. T., Lacelle, S., Bergeron, M. G., Beauchamp, D., and Carrier, D. (1996) *Chem. Phys. Lipids 83*, 131−140.
47. Lakey, J. H., and Ptak, M. (1988) *Biochemistry 27*, 4639−4645.

BI971793D